Applied Food Research 4 (2024) 100538

Contents lists available at ScienceDirect

Applied Food Research

journal homepage: www.elsevier.com/locate/afres

Enantioselective-GCxGC determination of α-terpinyl ethyl ether in wine: Quantitative analysis and identification of main terpene precursors

Aakriti Darnal [a,1], Alberto Ceccon [b,1], Martina Magni [b], Peter Robatscher [b], Simone Poggesi [c], Emanuele Boselli [a], Edoardo Longo [a,*]

[a] Faculty of Agricultural, Environmental and Food Sciences, Free University of Bozen/Bolzano, piazza Università 5, Bolzano 39100, Italy
[b] Laimburg Research Centre, Laimburg 6 - Pfatten (Vadena), Auer (Ora), BZ 39040, Italy
[c] Food Experience and Sensory Testing (Feast) Lab, Massey University, Palmerston North 4410, New Zealand

ARTICLE INFO

Keywords:
Wine classification
Enantioselective-GCxGC
Terpene chemistry
Olfactory attributes

ABSTRACT

The present study investigates the presence of α-terpinyl ethyl ether in wine and gives insights on the chemical processes leading to its formation. The analytical determination of (*S*)-α-terpinyl ethyl ether and (*R*)-α-terpinyl ethyl ether enantiomers was obtained by enantioselective comprehensive two-dimensional gas chromatography. Applying the two isomers as variables in combination with closely related terpenes, an accurate classification model of wines for the grape variety was successfully applied to a representative set of single-variety wine samples. Although presenting relatively low absolute concentrations, α-terpinyl ethyl ether (along with α-terpineol) resulted to be an inevitable and irreversible degradation product of linalool. In fact, a conversion study from enantiomerically pure (*R*)-linalool showed a major loss of the initial chiral configuration, i.e. only a very small enantiomeric excess characterized the product. α-Terpineol itself was also confirmed to be a precursor of α-terpinyl ethyl ether, however this process showed a smaller conversion over two weeks than from linalool, and without losses of the initial chiral configuration. In the real samples, the concentration of α-terpinyl ethyl ether was found to be much lower than that of α-terpineol, regardless of the alcohol-to-water ratio. Finally, olfactory descriptors were qualitatively attributed to each α-terpinyl ethyl ether enantiomer.

1. Introduction

Wine is an alcoholic beverage obtained from grapes, grape must, or grape juice (Chambers & Pretorius, 2010). Its complex chemical profile includes multiple chemical constituents, with different concentrations and impacts the sensory profile. Terpenes constitute a chemical class of volatile compounds with low or very low olfactory thresholds. Approximately forty terpenes have been identified in grapes (González-Barreiro et al., 2015). These exist as acyclic, monocyclic, or polycyclic molecules, the latter ones derived from the re-arrangement of acyclic precursors (Wedler et al., 2015). Terpenes contribute to resinous, fruity, and floral aromas in wine, and can undergo complex chemical reactions also after fermentation (Yang et al., 2023): for example, nerol can convert to limonene, terpinolene, linalool, and α-terpineol; geraniol can convert to β-ocimene, terpinolene, and linalool; linalool can convert into terpinolene. A related chemical class to that of the monoterpenols (e.g. α-terpineol, linalool, citronellol, linalool, nerol, hotrienol, and geraniol) are the terpene ethers. While some cyclic terpene ethers have been extensively studied in wine, such as 1,8-cineole (eucalyptol), *cis*- and *trans*-rose oxide, linalool-3,7-oxide (geranic oxide), and nerol oxide (Black et al., 2015), a few studies have reported the identification of (acyclic) terpene ethyl ethers in wine (linalyl, geranyl, and terpinyl ethyl ether). The object of this study is α-terpinyl ethyl ether, whose chemical structure is shown in Fig. 1. There is a lack of analytical validation for its identification, and there is also a lack of demonstrated pathways for its formation and information on its most likely precursors in wine.

Ethyl ethers of some monoterpenes such as linalyl, neryl, geranyl, and α-terpenyl ethyl ether were reported by Versini and co-workers (Carlin et al., 2016; Versini et al., 2008). According to these authors, these compounds could develop from glycosyl-conjugated forms into free forms through solvolysis, or *via* enzymatic reactions. α-terpenyl ethyl ether was also tentatively identified in wine in a few cases, i.e. in 'Manzoni Bianco' (Nicolini et al., 2003) and 'Riesling' (Blackford et al., 2022). Besides, its chemical precursors, the formation mechanism in

* Corresponding author.
E-mail address: edoardo.longo@unibz.it (E. Longo).
[1] These authors contributed equally

https://doi.org/10.1016/j.afres.2024.100538
Received 30 July 2024; Received in revised form 30 September 2024; Accepted 1 October 2024
Available online 2 October 2024

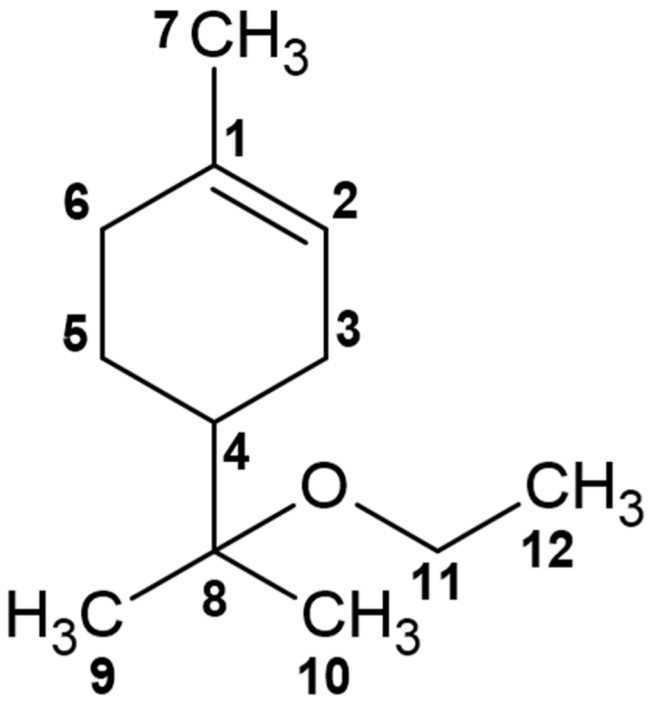

Fig. 1. Structure of α-terpinyl ethyl ether with carbon numeration according to Da Silva et al. (Da Silva et al., 2015).

wine, and its prevalent chiral configuration (see the stereogenic centre at C4, Fig. 1) have also not been yet evaluated. In particular, the sensory properties of terpene enantiomers can differ considerably: for example, (*S*)-α-terpineol is associated with 'resin' notes, whereas (*R*)-α-terpineol possesses a 'floral' character (*Sensory Properties of Optical Isomers | Perfumer & Flavorist*, n.d.; Tomasino et al., 2020). In addition, the enantiomeric ratio between couples of aroma-impacting enantiomers have been applied also as a quality and varietal marker in wine (Langen et al., 2016). Applying more species as variables in classification can increase the accuracy of classification models.

In this study, standards of (*S*)-α-terpinyl ethyl ether and (*R*)-α-terpinyl ethyl ether enantiomers were prepared and applied for quantitation in wine. A representative set of single-variety wines ('Gewürztraminer', 'Moscato Giallo', 'Moscato Bianco', 'Muscat of Alexandria', 'Kerner', 'Riesling', and 'Lacrima di Morro d'Alba') were analysed with enantioselective-GCxGC (enantioselective-GCxGC). A validated quantitation method was also applied. Each varietal sample set included wines from different producers, *terroir*, countries, and vintages. Finally, the main precursors of the formation of α-terpinyl ethyl ether are also presented, along with a qualitative determination of specific olfactory aroma attributes in wine for the two enantiomers.

2. Material and methods

2.1. Material

2.1.1. Chemicals

All chemical reagents and chemical standards ((*S*)-α-terpineol, (*R*)-α-terpineol, (*R*)-linalool, (*R*)-limonene, sodium hydride (in mineral oil), iodoethane, iodoethane-d5, (-)-α-pinene, (+)-α-pinene, (-)-β-pinene, linear saturated C8-C40 alkane standards series, anhydrous $MgSO_4$, NH_4Cl, NaCl), solvents (diethyl ether, petroleum ether, cyclohexane, ethyl acetate, ethanol, methanol, isopropanol - at LC grade purity or higher, and $CDCl_3$ containing 0.03 %v/v tetramethylsilane (TMS)), silica gel for flash chromatography (Supelco), and TLC plates (Supelco) were purchased from Merck Life Science S.r.l. (Milano, Italy). Ultrapure water was produced in-house with an Arium®Mini generator (Sartorius Italy S. r.l., Varedo, Italy).

2.1.2. Wine samples

Single-variety wine samples were directly purchased from local producers or web retailers. The complete list of single-variety wines analysed for this study is presented in Table 1. A neutral non-aromatic 'Pinot Blanc' wine was used as the quantification matrix. This wine was kindly donated by a local producer (Franz Haas Winery, Montagna, Bolzano, Italy). Basic oenological parameters of this 'Pinot Blanc' wine were: 1) alcohol by volume 14.00±0.05 $\%_{v/v}$, determined by distillation; 2) residual sugars < 0.1 $g{\cdot}L^{-1}$, determined by enzymatic analysis; 3) L-tartaric acid 1.6 ± 0.1 $g{\cdot}L^{-1}$, determined by enzymatic analysis; 4) L-malic acid 2.9 ± 0.1 $g{\cdot}L^{-1}$, determined by enzymatic analysis; 5) L-lactic acid 0.1 ± 0.1 $g{\cdot}L^{-1}$, determined by enzymatic analysis; 6) total polyphenols 292±1 $g_{GAE}{\cdot}L^{-1}$, determined by Folin assay (gallic acid equivalents); 7) total-SO_2 61 ± 1 $mg{\cdot}L^{-1}$, determined by colorimetric analysis; 8) free-SO_2 2 ± 1 $mg{\cdot}L^{-1}$, determined by colorimetric analysis; 9) acetic acid 0.34±0.01 $g{\cdot}L^{-1}$, determined by enzymatic analysis; 10) pH 3.3 ± 0.1, determined with a pH meter.

2.2. Methods

2.2.1. Chemical synthesis

In Supporting Information **PART I** (**Paragraph I.1, I.2, I.3** and **Figure SI I-1,2,3**), the synthesis protocol is fully detailed, along with all the related analytical characterizations. All isolated and purified products appeared as very clear, transparent, non-coloured, and non-viscous oils at room temperature. The recovered purified products weighed: 1) (*S*)-α-terpinyl ethyl ether = 0.31 g (yield = 26 %), 2) (*R*)-α-terpinyl ethyl ether = 0.31 g (yield = 26 %), 3) (*S*)-α-terpinyl ethyl-d5 ether = 0.35 g (yield = 30 %), respectively. The purified products were all characterized analytically (see Supporting Information **PART II** (**Paragraph II-1,2,3**)).

2.2.2. HS-SPME-enantioselective-GCxGC-ToF/MS analysis

For the analyses, 3 mL of wine sample was placed in a 10-mL SPME vial along with 0.5 g of NaCl and 1 mL of ultrapure water. To this mixture, 2 μL of a stock of pure (*S*)-α-terpinyl ethyl-d5 ether (75 $mg{\cdot}L^{-1}$ in ethanol) and 20 μL of ultrapure water were added. Then the vial was sealed with a metal cap with a perforable silicon septum. The HS-SPME-enantioselective-GCxGC-ToF/MS analysis was carried out on a GCxGC Agilent 7890B coupled with a ToF/MS Pegasus® Flux BT 4D mass spectrometer (LECO Corporation, Germany) employing a MEGA-DEX G-01 30 m x 0.25 cm x 0.25 μm (MEGA S.r.l, Italy) as the first dimension chiral stationary phase and a MEGA-17 MS Sil phase (MEGA S.r.l, Italy) 1.0 m x 0.1 μm x 0.10 mm as the second dimension (non-chiral) stationary phase. The HS-SPME procedure was adapted from a published protocol (Khvalbota et al., 2021). Each sample was conditioned at 60 °C for 30 min under 500 r.p.m. stirring, and then a pre-conditioned SPME fibre (1 cm, DVB/CAR/PDMS, 50/30 μm SPME fibre, Supelco) was exposed into its headspace for 30 min at 60 °C under 500 r.p.m. stirring. GCxGC-ToF/MS parameters: helium flow rate = 1 $mL{\cdot}min^{-1}$; temperature program = 40 °C for 6 min, 2 $°C{\cdot}min^{-1}$ to 145 °C, followed by 5 $°C{\cdot}min^{-1}$ to 230 °C; secondary oven DT = + 5 °C; transfer line temperature = 250 °C; ion source EI energy = 70 eV; spectral acquisition range = m/z 35 - m/z 530; extraction frequency = 32 kHz; acquisition rate = 150 $spectra{\cdot}s^{-1}$; modulation period = 2.0 s, and injection time = 80 ms. The resulting resolution for the two α-terpinyl ethyl ether enantiomers in the first dimension was 2.11 (the (*S*) isomer eluting earlier than the (*R*) isomer). The assignment was based on the elution and spectral profiles of the injected reference standards ((*S*)-α-terpinyl ethyl ether, (*R*)-α-terpinyl ethyl ether, (*S*)-α-terpinyl ethyl-d5 ether, (*R*)-α-terpineol, (*R*)-linalool, and (*R*)-limonene). Retention indexes were calculated against the C8 – C40 linear alkanes series (solution in dichloromethane, Supelco). For the determination of the purity of the synthesized products, the same conditions described herein were

Table 1
Analysed single-variety wines.

Sample	Grape Variety	Vintage	Origin	Winery	Notes
GT-1		2016	Trentino, Italy	Mezzacorona	
GT-2	'Gewürztraminer'	2018	South Tyrol, Italy	Tramin	
GT-3		2019			Different vineyards but the same producer
GT-4		2019		Local winery	
GT-5		2019			
GT-6		2019			
GT-7		2019			
GT-8		2019			
GT-9		2019			
GT-10		2019		Kellerei Bozen	
GT-11		2020	Alsace, France	Fernand Engel	
GT-12		2020		Domaine Zind-Humbrecht	
GT-13		2021		Pierre Frick	Orange-wine style
GT-14		2021		Alsace Willm	
GT-15		2022		Gruss	
GT-16		2022		Charles Sparr	
KE-1		2021		Villscheider, Eisacktal	
KE-2	'Kerner'	2022	South Tyrol, Italy	Cortaccia	
KE-3		2022		Eisacktal	
KE-4		2022		Weingut Niklas	
KE-5		2022	Trentino, Italy	Cantina Micheli	
KE-6		2022	South Tyrol, Italy	Griesserhof, Eisacktal	
KE-7		2022	Trentino, Italy	Zanotelli wines	
KE-7		2022	South Tyrol, Italy	Kellerei Bozen	
KE-8		2022		Stiftskellerei Neustift	
LM-1	'Lacrima di Morro d'Alba'	2020	Marche, Italy	Filodivino	
LM-2		2020		Velenosi	
LM-3		2021		Piergiovanni Giusti	
LM-4		2020		Marotti Campi	
LM-5		2021		Marotti Campi	
LM-6		2022		CasalFarneto	
LM-7		2022		Marotti Campi	
LM-8		2021		Mancinelli	
MB-1		2019	Veneto, Italy	Alla Costiera	
MB-2	'Moscato Bianco'	2022	Sicily, Italy	Cantina Marilina	Macerated on the skins
MB-3		2022	Apulia, Italy	Maccone	
MB-4		2022	Piedmont, Italy	Bersano	
MA-1		2021	Pantelleria, Sicily, Italy	Costaviola	
MA-2	'Muscat of Alexandria'	2022		Cantine Pellegrino	
MA-3		2022		Donnafugata	
MA-4		2022	Sicily, Italy	Cantine Florio	
MA-5		2022		Nicosia	
MG-1	'Moscato Giallo'	2020	Trentino, Italy	Vallarom	
MG-2		2022	South Tyrol, Italy	Tramin	
MG-3		2022		Brigl	
MG-4		2022		Colterenzio	
MG-5		2022		Alois Ladeger	
MG-6		2022	Trentino, Italy	Cantina Aldeno	
MG-7		2015		Cavit	
RI-1		2020	Rheingau, Germany	Franz Künstler	
RI-2	'Riesling'	2020	South Tyrol, Italy	Laimburg	
RI-3		2021		Villscheider, Eisacktal	
RI-4		2021	Rheinland-Pfalz, Germany	Wachtenburg	
RI-5		2021	Alsace, France	Charles Sparr	
RI-6		2022	Mosel, Germany	Dr Fischer	
RI-7		2022	South Tyrol, Italy	Colterenzio	
RI-8		2021		Pacher Hof	

applied, except that the analyses were conducted in 1D mode (i.e., applying with no modulation) [inlet split ratio = 25:1, detector solvent delay = 10 min, acquisition rate = 5 spectra·s^{-1}, and liquid injection volume in cyclohexane = 0.25 μL - the specific injected concentrations are reported in the respective paragraphs in the Supporting Information].

2.2.3. Quantitation methods and validation

Calibration standards: Reference concentrations of (*R*)-limonene, (*R*)-linalool, (*R*)-α-terpinyl ethyl ether, and (*R*)-α-terpineol were applied for the calibration (see instrumental conditions in paragraph 2.2.2). (*R*)-limonene, (*R*)-linalool, (*R*)-α-terpinyl ethyl ether, and (*R*)-α-terpineol were utilized as external standards also to quantitate the relative (*S*)-isomers (assuming identical response factors). Each calibration standard and accessory analysis (e.g. evaluation of method's robustness, intra-day, and inter-day precisions, recoveries, etc.) were analysed in triplicates (or in quintuplicates, where stated). **Calibration matrix:** The neutral non-aromatic 'Pinot Blanc' (see paragraph 2.1.2 - Wine samples) was applied as the calibration matrix. A GCxGC analytical ion-chromatogram (AIC) trace of this wine (not spiked) is compared with the same wine after spiking (**Figure SI II-12**). Each sample was spiked also with 2 μL of a 75 mg·L^{-1} solution of (*S*)-α-terpinyl ethyl-d5 ether in ethanol. **Matrix effect:** Wines from different varieties possess different matrix components, that might influence the response factors of the analytes; for this reason, for each set of wines characterized by the same grape variety, a mix (1 mL each) of all samples in the varietal group was prepared. The resulting pooled sample (herein called "mix") was then spiked at two different calibration levels with the calibration standards

and with the deuterated analogue, as aforementioned. These varietal mix samples were then analysed: the concentration differences between the recovered concentrations in the spiked and non-spiked mix samples were then compared with the same concentrations spiked in the neutral 'Pinot Blanc' matrix. The significance of this difference ($\alpha = 0.05$) was applied as an estimator of the effect of (varietal) matrix interference. **Robustness** (for changes in ABV%): The robustness of the method was tested against differences in the ethanol content of wine (ABV%). The 'Pinot Blanc' wine used as a calibration matrix was prepared in a 3:1 mix with (A) water (as for the calibrations) or (B) different hydroalcoholic solutions, to reach different final desired ABV% (see SI, **Table SI II-3**). **Recovery:** The recoveries were determined by spiking two different standard concentrations in triplicates in the 'Pinot Blanc' wine matrix, and by repeating this determination on three different days. The reference concentrations selected for estimating the recovery were not the same as those used for calibration.

Parameters of the quantitation models: The parameters obtained from the calibration models (linearity, precision, limit of detection, limit of quantitation, recovery, robustness against differences in the initial ethanol content, and significance of deviations due to varietal matrix effect) are reported in the SI (**Table SI II1 - Table SI II4**).

2.2.4. Flow-injection atmospheric-pressure chemical ionization (APCI)-(HR)MS

Characterization of intact molecular ions: APCI-(HR)MS was applied for the detection of the intact molecular ions (of the synthesized products). The applied method was adapted from the literature (Gao et al., 2012). The analyses were performed on an Orbitrap Exploris 240 Mass Spectrometer (Thermo-Fisher Scientific, Rodano, Milano, Italy) equipped with an APCI ion source. The analyses were run in flow-injection mode (flow rate of 50 $\mu L \cdot min^{-1}$). Reference concentrations of the compounds were prepared in cyclohexane at a concentration of 10 $mg \cdot mL^{-1}$ or 40 $mg \cdot mL^{-1}$. APCI-(HR)MS parameters: vaporizer temperature = 250 °C (the two isomers) or 200 °C (deuterated analogue), capillary temperature = 300 °C, sheath gas (N_2) flow rate = 30 (arbitrary units), auxiliary flow rate = 15 (arbitrary units), and sweep gas flow rates = 1 (arbitrary units). Positive ionization mode was applied, with ionization discharge current = 8 μA, and RF lens = 70 %, working resolution = 240,000 at *m/z* 200, acquisition rate = 1.5 (s)$^{-1}$. **MS/MS fragmentations**: For the APCI-MS/MS analysis, a 0.4 Da isolation width was applied to the quadrupole, with collision energy = 10 V. Nitrogen was used as collision gas. The spectra of each analyte are reported as average over at least 20 s (**Figure SI II-2, Figure SI II-6 and Figure SI II-9**). Tentative assignments of the fragmentation patterns are also presented in SI (**Figure SI II-3** and **SI II-10**).

2.2.5. Nuclear magnetic resonance spectroscopy (NMR)

2.2.5.1. Preparation of NMR samples. Solutions of (*S*)-α-terpinyl ethyl ether, (*R*)-α-terpinyl ethyl ether, (*S*)-α-terpinyl ethyl-d5 ether, and (*R*)-α-terpineol were prepared by dissolving the respective compound in 1 mL of $CDCl_3$ (containing 0.03 $\%_{v/v}$ TMS as internal standard) to reach a concentration of 25 mM.

2.2.5.2. Acquisition and processing of monodimensional (1D) and bidimensional (2D) nuclear magnetic resonance (NMR) spectra. All NMR experiments were carried out at 25 °C using a 600 MHz spectrometer (JNM-ECZ from JEOL Ltd., Tokyo, Japan), equipped with a room temperature "Royal" HFX/FGSQ probe. All 1D ^{1}H NMR experiments were acquired with the following parameters: acquisition time (AQ) = 5.4 s, spectrum width (SW) = 10 ppm, frequency offset = 4 ppm, 90° ^{1}H pulse = 7.1 ms, receiver gain = 56, dummy scans = 4, number of scans (NS) = 8 and relaxation delay of 40 s. A DANTE pulse trains sequence was added to remove any signal coming from residual water. Complete chemical shift assignments of the synthetised molecules were achieved by: a) 1D ^{13}C DEPTQ experiments (Burger & Bigler, 1998) recorded with SW = 160 ppm, frequency offset = 70 ppm, NS = 6000 and relaxation delay of 2 s, b) ^{1}H–^{13}C HSQC-TOCSY and c) ^{1}H–^{1}H NOESY experiments were acquired NS = 256 and 48, respectively, and were obtained with 1024 and 256 points in the direct and indirect dimensions, respectively. Mixing times of 50 ms and 500 ms were used for the 1H-13C HSQC-TOCSY and 1H-1H NOESY, respectively. The same 25 % poisson-gap Non-Uniform Sampling (NUS) schedule was used for ^{1}H–^{13}C HSQC-TOCSY and ^{1}H – ^{1}H NOESY experiments. Spectra reconstruction as well as NMR data processing and analysis were conducted with Delta NMR Data Processing software (JEOL Ltd., Tokyo, Japan). For 1D ^{1}H NMR experiments an exponential window function was employed with a line broadening factor of 0.2 Hz and zero-filled to 2x number of acquisition points prior to Fourier transformation. Each spectrum was then manually phase-corrected and baseline-corrected. For 2D NMR experiments, an exponential window function with a line broadening of 5 Hz was employed on both indirect and direct dimensions. All chemical shifts were calibrated relative to the chemical shift of TMS.

2.2.6. Fourier-transform infrared spectroscopy (FTIR)

The FTIR spectra were recorded in transmittance mode on a Tensor 27 infrared spectrometer (Bruker). The background was measured before each analysis and automatically subtracted. Data were collected with 2 cm^{-1} resolution, 64 scans per sample, and 4000–400 cm^{-1} scan range. For each analysis, ca. 5 μL of pure standard was used.

2.2.7. Qualitative determination of olfactory attributes

Eight expert panellists (age 20 – 40, 3 males, 5 females) performed an olfactory (orthonasal) assessment of the spiked enantiomers in a temperature-controlled room. The panel was asked to qualitatively evaluate the compounds spiked separately in the Pinot Blanc wine (30 mL *per* sample in ISO glasses) at four different concentrations: very high (120 $mg \cdot L^{-1}$), high (12 $mg \cdot L^{-1}$), medium (1.2 $mg \cdot L^{-1}$), and low (0.12 $mg \cdot L^{-1}$). (*S*)-α-terpineol and (*R*)-α-terpineol were used for comparison as reference odorants at the same concentrations. The non-spiked 'Pinot Blanc' wine was used as a reference control for each compound-spiked 'Pinot Blanc' wine. Panellists had to smell and qualitatively describe the samples. Then, the frequency of citation for each attribute was generated. The synthetic nature of the compounds, although produced in very pure form and being already present in wine, prevented any gustatory assessment of the spiked wines, in agreement with the available literature and safety precautions (Falcao et al., 2012; Pineau et al., 2007). Protocols involving qualitative direct assessments of olfactory attributes of synthetic compounds were considered for designing the applied methodology (Büyükbayram et al., 2024; Gilles & Antoniotti, 2022; Li et al., 2014; Qin et al., 2024; Uehara & Baldovini, 2021; Zhu et al., 2021). Accordingly, only olfactory detection tests were performed, as considered to carry very low to no risks. For this reason, approval from an ethical committee was not required, in line also with the above-cited published works. In addition, no personal data were used for the statistical analysis or individual profiling, and the identity of the panellists was not disclosed to ensure their privacy. All of the participants were given full information beforehand on the task they would perform and were asked to sign a written informed consent before the study. They were also informed on how their data would be processed.

2.2.8. Statistical analysis

The statistical analysis was performed with XLStat Premium (version 2023.2.1414, Addinsoft, New York, NY, USA). One-way ANOVA with Tukey's *post-hoc* test was applied ($\alpha = 0.05$). For multivariate analysis, all the applied variables were first $\log_{10}$-transformed and then autoscaled (first mean-centered, then scaled to unit variance). The linear discriminant analysis (LDA) model was re-calculated eleven times, each time with *prior* independent randomization and random extraction of a representative training set and validation set (the latter one containing always nine samples). A stepwise algorithm was used, applying a

tolerance of 0.001, imposing equality of the covariance matrices and *prior* probabilities. For LDA, all Muscat samples were grouped together. The classification results (% of correct predictions in training and in validation) are presented as averages over the eleven runs. Missing values were estimated with Nonlinear Iterative Partial Least Squares (NIPALS) algorithm. An online free word cloud generator (https://worditout.com/word-cloud/create, retrieved data November 11th 2023) was used for the sensory data analysis.

3. Results and discussion

3.1. Identification of α-terpinyl ethyl ether in wine

In some previous studies (Poggesi et al., 2022), a GCxGC-MS feature was observed in the headspace of various wines, with particular strong relative abundances in some aromatic wines (e.g. from 'Muscat' cvs.); this feature presented an EI-MS (EI = 70 eV) spectrum similarl to that of α-terpineol, except for a *m/z* 87 fragment (not present in the EI-MS spectrum of α-terpineol) (**Figure SI II-1** and **Figure SI II-5**) and a completely different elution profile with respect to that of α-terpineol in GCxGC. Eventually, the only candidate matching all observations (elution profile, MS spectrum) was the compound α-terpinyl ethyl ether. Few studies already tentatively reported its identification in wine. Blackford et al. associated the presence of monoterpenol ethyl ethers with the fermentation and extraction of grape skins (Blackford et al., 2022). In another published study (Keyzers & Boss, 2010), linalyl ethyl ether and α-terpinyl ethyl ether in wine were identified tentatively. Another study tentatively identified α-terpinyl ethyl ether in the volatile profile of 'Manzoni Bianco' (Nicolini et al., 2003). A 1983 study focused on the formation of ethyl ethers during distillation (Strauss et al., 1985a; Strauss & Williams, 1983). Ethyl ether derivatives of monoterpenols and monoterpendiols were then also proposed in wine (Strauss et al., 1985b). Those studies suggested a possible formation of these compounds *via* ethanolysis of suitable terpene precursors. However, considering the first reported detection of α-terpinyl ethyl ether over distillation, and also reports showing the presence of monoterpenol ethyl ethers in hop oil after hop boiling (Praet et al., 2015), a possible explanation for its formation could be the application of heat: heat treatments also occur during the analytical procedure (e.g. the SPME fibre desorption in the heated GC inlet). The SPME fibre composite chemistry as well might have induced such chemical transformations on suitable terpene precursors. As no report has yet explored this possibility concerning the formation of α-terpinyl ethyl ether, a preliminary test was done in this study on an aromatic wine that had already shown the presence of that compound: we had hypothetically considered that heat processes in the presence of ethanol and suitable precursors might cause the formation of the ethyl ether; however, we have also considered that a similar concentration (to ethanol) of added methanol or isopropanol should cause the formation of the relative methyl or isopropyl ether, as well. In detail, a sample of wine that already showed the presence of α-terpinyl ethyl ether was added with an equimolar (to ethanol) amount of methanol or isopropanol. As a result, the analysis runs immediately after these additions did not show any new analytical features that could be associated with a methyl or isopropyl ether, but still showed the presence of α-terpinyl ethyl ether (*data not shown*). Finally, a test on the same wine was done in static headspace mode (thus avoiding the SPME procedure): this test clearly indicated that no chemical reaction promoted by the triphasic fibre chemistry was a cause for the detection of α-terpinyl ethyl ether in GCxGC, as the feature was present in the chromatograms both with and without applied SPME.

Furthermore, no information was available in the literature on the enantiomeric separation of the α-terpinyl ethyl ether enantiomers (stereogenic centre at C4, see Fig. 1). Therefore, to analytically test and confirm the presence of α-terpinyl ethyl ether in wine, to assess for the presence of a prevalent enantiomer or of a close-to racemic mixture, and to also provide a qualitative determination of their sensory attributes in wine, enantiomerically pure reference standards were obtained by synthesis (see next paragraph).

As a final note, on an achiral polar PEG stationary phase used in preliminary tests (Poggesi et al., 2022), α-terpinyl ethyl ether's retention index was 1432 (for comparison, ethyl octanoate has a retention index of 1440 on the same column): without the enhanced resolution capability of GCxGC, this feature (even without chiral separations) would be very difficult to observe in wine.

3.2. Synthesis of α-terpinyl ethyl ether enantiomers

Despite being technically simple and cheap to perform, and with large conversions in a few hours, acidic synthetic routes to α-terpinyl ethyl ether, for instance from limonene or pinene (Catrinescu et al., 2015; Da Silva et al., 2015; da Silva et al., 2020; Hensen et al., 1997; Polo et al., 2019) were ruled out as the cause of racemization and isomerization. Indeed, our preliminary trials from (+)-α-pinene, (-)-α-pinene, and (-)-β-pinene as starting reagents in acidic conditions proved this to be an unsuitable option (*data not shown*). Consequently, a tailored Williamson ether synthesis approach was selected and optimized, starting directly from the pure (*S*)-α-terpineol and (*R*)-α-terpineol precursors. All details of the synthesis protocol are provided in the Material and Methods and the Supporting Information. The reaction temperature resulted in the most critical parameter to achieve an acceptable reaction rate and yield, due to the slow reactivity of the α-terpineol tertiary alcohol and the derived tertiary α-terpinyl alkoxide. Anhydrous 1,4-dioxane was selected as the best solvent, as it allowed much higher conversions in more reasonable reaction times than other tested conditions (*data not shown*), with a final yield of ca. 30 % for all isolated and purified products. The obtained products were fully characterized analytically (see Supporting Information).

3.3. enantioselective-GCxGC separation of the α-terpinyl ethyl ether enantiomers

After confirmation of the purity of the synthesized products by the application of mono-dimensional GC (PEG polar stationary phase) and GCxGC (PEG polar x mid-polar stationary phases), an attempt was made at the separation of the two enantiomers on a chirally-derivatized stationary phase (mid-polar phase with a 30 % heptakis (2,3-di-O-methyl-6-O-t-butyl dimethylsilyl)-β-cyclodextrin derivatization). No enantiomeric separation was observed (see **Figure SI II-13**). A careful columns screening (see the Material and Methods section) managed to successfully identify a column consisting of a γ-cyclodextrin chirally-derivatized mid-polar stationary phase (MEGA-DEX G-01 30 m x 0.25 cm x 0.25 μm) that allowed a chiral resolution > 2 between the two enantiomers. The extracted ion chromatogram (XIC) traces showing the 2D and 1D features for the resolved linalool enantiomers, for (*S*)-α-terpinyl ethyl-d5 ether, for the resolved α-terpinyl ethyl ether enantiomers, and the resolved α-terpineol enantiomers are reported in **Figure SI II-14**.

The calculated linear retention indexes (determined against C8 – C40 linear saturated alkane standards) on this γ-cyclodextrin chirally-derivatized column, applying the optimized instrumental setup (see Material and Methods) for (*S*)-α-terpinyl ethyl ether, (*R*)-α-terpinyl ethyl ether, and (*S*)-α-terpinyl ethyl-d5 ether were 1306, 1311, and 1303, respectively.

3.4. NMR

The 1D ^{1}H NMR spectra of (*S*)-α-terpinyl ethyl ether, (*R*)-α-terpinyl ethyl ether, and (*S*)-α-terpinyl ethyl-d5 ether are shown in Fig. 2A, B and C, respectively. For (*S*)-α-terpinyl ethyl ether and (*S*)-α-terpinyl ethyl-d5 ether, complete and unambiguous assignments of ^{1}H and ^{13}C resonances were achieved using a combination of ^{1}H, ^{13}C HSQC (**Figure SI II-15A, C**), ^{13}C DEPTQ (**Figure SI II-15B, D**) and ^{1}H, ^{13}C HSQC-TOCSY experiments (**Figure SI II-16A, B**). As expected, 1D ^{1}H spectrum (Fig. 2C) and

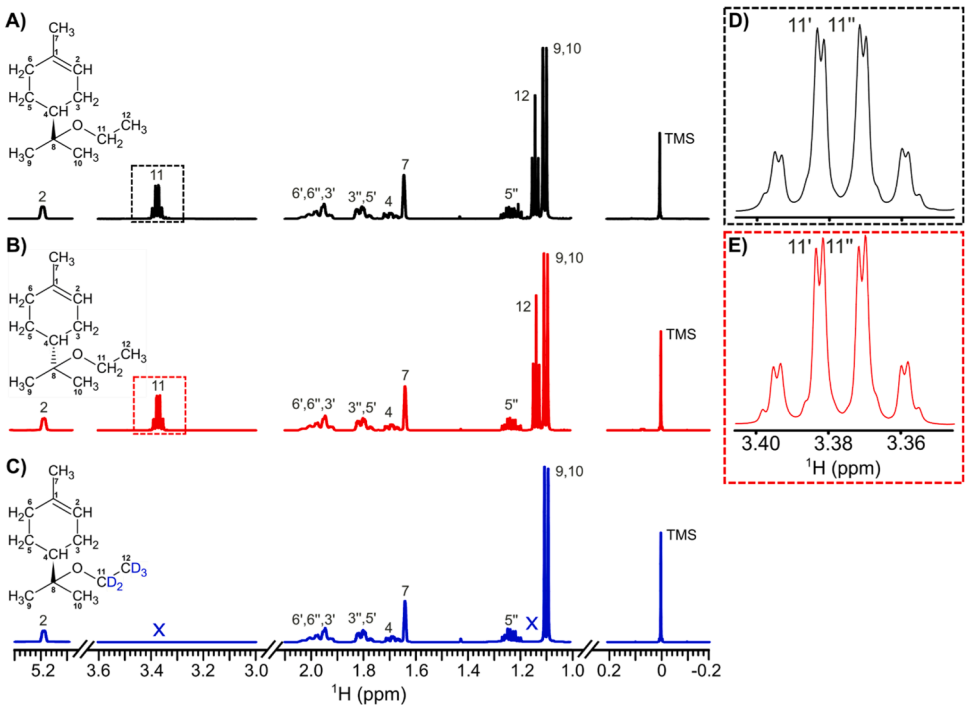

Fig. 2. ^{1}H NMR spectra (600 MHz, $CDCl_3$, $T = 25$ °C) of 25 mM (A) (*S*)-α-terpinyl ethyl ether, (B) (*R*)-α-terpinyl ethyl ether and (C) (*S*)-α-terpinyl ethyl-d5 ether. The assignments of the chemical shifts are shown in the spectra (numbering refers to the atom position in the molecules – left-hand side). Signals corresponding H11' and H11" are boxed in the spectra and zoomed in (D) and (E) for (*S*)-α-terpinyl ethyl ether and (*R*)-α-terpinyl ethyl ether, respectively. TMS = tetramethylsilan.

the corresponding 2D ^{1}H, ^{13}C HSQC spectra (**Figure SI II-15C**) lack the signals corresponding to methylene and methyl protons of the ethyl ether segment since deuterons are invisible to NMR probes tuned to ^{1}H. Additionally the 1D ^{1}H NMR spectra of the two enantiomers, (*S*)-α-terpinyl ethyl ether (Fig. 2A) and (*R*)-α-terpinyl ethyl ether (Fig. 2B) overlap. However, the two methylene protons in the ethyl ether moiety are diastereotopic. This produced slightly different chemical shifts of both quartet signals from H11' and H11" (see Fig. 2D and 2E). The resolution of the two protons is beyond the scope of this paper; however, we noted that the intensity of the two sets of signals is not equivalent due to different relaxation rates (T_2 or T_1) or a dipolar interaction with nearby nuclei. Therefore, 2D NOESY was applied to determine the orientation and spatial arrangement of the ethyl ether segment relative to the cyclohexene ring. A NOE between H11 of the ethyl ether CH_2 and

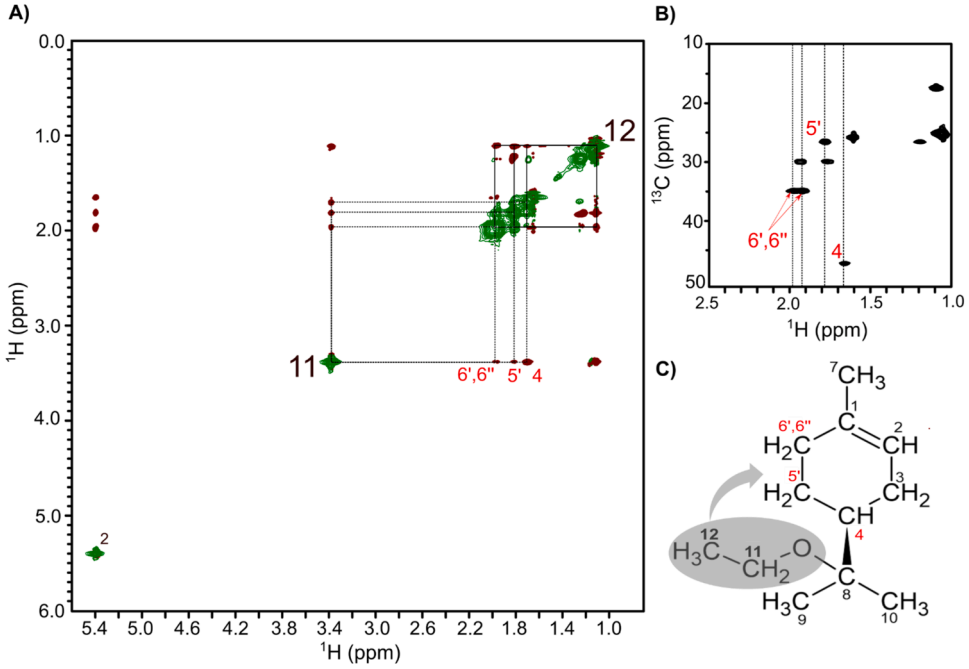

Fig. 3. Orientation of the ethyl ether segment in the (*S*)-α-terpinyl ethyl ether molecule: (A) 1H,1H NOESY spectrum of 25 mM (*S*)-α-terpinyl ethyl ether acquired at 600 MHz, $T = 25$ °C; (B) Portion of the 1H, 13C HSQC spectrum with the assignments of H4, H5' and H6', H6" (see molecule shown in C); (C) Scheme of (*S*)-α-terpinyl ethyl ether molecule indicating the NOE correlations observed in the NOESY experiment.

H4, H5', H6', and H6' of the ring was observed (Fig. 3), suggesting a specific positioning of the ethyl ether segment opposite to the double-bond side of the cyclohexene ring (Fig. 3C).

3.5. Quantitative determination of α-terpinyl ethyl ether enantiomers and other terpenes species in wine

The quantitation method was applied to the wines reported in Table 1, and the quantitation results for α-terpinyl ethyl ether enantiomers and other related terpenes are reported in Table 2. The parameters of the validated calibration method are thoroughly presented in the SI (**Table SI II-1–4**). Limonene in the wines showed no signals ≥ LOQ and most samples were < LOD (visually observed with respect to the background noise after XIC extraction for *m/z* 68), or even showed no observable signal at all. As a consequence, limonene isomers are not discussed. Similarly, samples in which both α-terpinyl ethyl ether

Table 2
Quantitation results for α-terpinyl ethyl ether enantiomers and related terpene species. Samples presenting abundances < LOQ for both enantiomers are not reported in the Table, for brevity.

Wine	(*S*)-α-terpinyl ethyl ether (± 0.0002 mg·L^{-1})	(*R*)-α-terpinyl ethyl ether (± 0.0002 mg·L^{-1})	(*S*)-linalool (± 0.001 mg·L^{-1})	(*R*)-linalool (± 0.001 mg·L^{-1})	(*S*)-α-terpineol (± 0.0007 mg·L^{-1})	(*R*)-α-terpineol (± 0.0007 mg·L^{-1})
KE-1			<LOQ	<LOQ	0.039	0.146
KE-2			0.002	0.013	0.063	0.147
KE-3	0.0011	0.0010	0.036	0.036	0.101	0.169
KE-4	0.0021	0.0018	<LOQ	<LOQ	0.070	0.144
KE-5			<LOQ	<LOQ	0.061	0.169
KE-6			<LOQ	<LOQ	0.046	0.148
KE-7			<LOQ	<LOQ	0.040	0.130
KE-8			<LOQ	<LOQ	0.044	0.122
KE-9	<LOQ	0.0007	<LOQ	<LOQ	0.045	0.134
RI-1	<LOQ	0.0009	<LOQ	<LOQ	0.063	0.120
RI-2			<LOQ	<LOQ	0.020	0.069
RI-3			<LOQ	<LOQ	0.028	0.086
RI-4			<LOQ	<LOQ	0.039	0.121
RI-5			<LOQ	<LOQ	0.022	0.081
RI-6			<LOQ	<LOQ	0.021	0.076
RI-7	<LOQ	0.0007	<LOQ	<LOQ	0.079	0.137
RI-8			<LOQ	<LOQ	0.008	0.067
MB-1	0.0085	0.0083	0.124	0.180	0.529*	0.543*
MB-2	0.0023	0.0020	0.007	0.003	0.258*	0.320*
MB-3	0.0079	0.0072	<LOQ	<LOQ	0.360*	0.366*
MB-4	<LOQ	0.0015	0.002	0.030	0.203	0.321*
MA-1	0.0022	0.0020	0.005	0.010	0.288*	0.265*
MA-2	0.0069	0.0048	0.426*	0.457*	0.265*	0.211
MA-3	0.0048	0.0045	0.279*	0.311*	0.810*	0.753*
MA-4	0.0036	0.0030	<LOQ	0.001	0.229	0.237
MA-5	0.0100	0.0041	1.869*	0.900*	0.542*	0.405*
MG-1			<LOQ	<LOQ	0.103	0.144
MG-2	0.0054	0.0045	0.237	0.238	0.421*	0.386*
MG-3	0.0011	0.0018	0.151	0.111	0.210	0.193
MG-4	0.0024	0.0019	0.131	0.187	0.235	0.201
MG-5	0.0063	0.0043	0.589*	0.320*	0.300*	0.247
MG-6	0.0013	0.0010	0.112	0.098	0.549*	0.521*
MG-7	0.0011	<LOQ	<LOQ	<LOQ	0.141	0.154
GT-1			<LOQ	<LOQ	0.031	0.102
GT-2			<LOQ	<LOQ	0.057	0.085
GT-3			0.122	0.179	0.090	0.107
GT-4			0.108	0.071	0.098	0.104
GT-5			0.003	0.035	0.030	0.045
GT-6			0.058	0.007	0.031	0.062
GT-7			0.188	0.191	0.084	0.076
GT-8	<LOQ	0.0009	0.383*	0.319*	0.123	0.133
GT-9	<LOQ	0.0007	0.246	0.258*	0.078	0.086
GT-10			<LOQ	<LOQ	0.036	0.065
GT-11			<LOQ	<LOQ	0.010	0.026
GT-12			0.006	0.003	0.038	0.042
GT-13	0.0015	<LOQ	0.094	0.174	0.195	0.137
GT-14			<LOQ	<LOQ	0.011	0.033
GT-15			<LOQ	<LOQ	<LOQ	0.014
GT-16			<LOQ	<LOQ	0.019	0.031
LM-1			<LOQ	<LOQ	0.056	0.063
LM-2	0.0013	<LOQ	0.002	0.005	0.080	0.130
LM-3			<LOQ	<LOQ	0.036	0.057
LM-4			<LOQ	<LOQ	0.022	0.054
LM-5			<LOQ	<LOQ	0.017	0.031
LM-6			<LOQ	0.001	0.046	0.027
LM-7			0.002	0.002	0.021	0.044
LM-8			<LOQ	<LOQ	0.048	0.053

KE1–6: Kerner, RI1–8: Riesling, MB1–4: Moscato Bianco, MA1–5: Muscat of Alexandria, MG1–7: Moscato Giallo, GT1–16: Gewürztraminer, LM1–8: Lacrima di Morro d'Alba.

* Estimated value exceeding the tested linear range. LOQ for both α-terpinyl ethyl ether enantiomers was calculated as 0.0007 mg.L^{-1} (as 10σ·slope^{-1}). See **Table SI II-1** in the Supporting Information for more details.

enantiomers were < LOQ are not reported in Table 2 for brevity.

Despite many samples presenting concentrations < LOQ for α-terpinyl ethyl ether isomers (24 out of 58 samples), almost all samples showed traces above the LOD. Therefore, to enable a comprehensive view, a one-way ANOVA (α = 0.05) for the variety was applied directly to the measured relative abundances (i.e. measured peak areas) instead. (*R*)-limonene, (*S*)-α-terpinyl ethyl ether, (*R*)-α-terpinyl ethyl ether, and (*R*)-α-terpineol in 'Muscat of Alexandria' and 'Moscato Bianco' wines were significantly higher than in the rest of the wines. (*S*)-α-terpineol in all 'Muscat' wines was significantly higher as well. Among 'Kerner', 'Gewürztraminer', 'Riesling', and 'Lacrima di Morro d'Alba' wines, no significant differences were found. Then, a principal component analysis (PCA) model was built based again on the relative abundances. The peak areas were considered instead of the derived absolute concentrations as most of the samples showed signals < LOQ but > LOD, so they would need to be estimated (e.g. in a multivariate way, for example with NIPALS) for the PCA. This could likely result in the introduction of bias, as the data matrix reconstruction heavily relies on the present values. Conversely, the direct application of the peak areas (when still > LOD), involving much fewer missing values to be estimated and consequently more available samples, would cause just a limited increase in the random error added into the model. By definition, random error can affect only very slightly the projections of the major trends present in the data onto the first principal components. In addition, the PCA model was calculated on the correlation matrix, which involves auto-scaling of each original variable to unit variance: any multiplication factor (such as the calibration slope) would therefore correspond to an effect/trend that is removed by the auto-scaling even before the PCA model is calculated.

For building the PCA model, all peak areas were first $\log_{10}$-transformed, to reduce the differences in internal variance ("within-group") between the different variety groups. The obtained PCA model is presented in Fig. 4. The enantiomeric excesses (for linalool, α-terpinyl ethyl ether, and α-terpineol pairs), are projected as supplementary variables (the enantiomeric excess values are reported in **Table SI II-5**).

Despite the applied log-correction and auto-scaling, the cumulative explained variance for the first two PCs was 90.47 % (Fig. 4). Samples from the same variety were almost always clustered closely in the PC1 vs. PC2 projection, albeit often different varieties partially overlapped. Homogenous groups for the same variety can be observed for 'Gewürztraminer', 'Muscat', and 'Kerner', although these groups are often contiguous to or overlapping with each other. All the 'Muscat' wines (except for the MG-1 outlier) were separated from the other groups. 'Riesling' and 'Lacrima di Morro d'Alba' groups were divided into various distinct clusters, separated along a PC1 vs. PC2 diagonal projection. To the best of our knowledge, no previous study has yet investigated the enantiomeric distribution of the terpenes in 'Lacrima di Morro d'Alba' wines (from Marche region - Central Italy). Its peculiar anthocyanins profile has been instead well characterized, hinting also at a possible origin of this grape variety from an ancient inter-specific hybridisation (Boselli et al., 2008). 'Muscat' wines presented the highest contributions from all the analysed compounds. This was also seen previously in other reports (Furdíková et al., 2021), where 'Muscat' wines showed a richer volatile profile, namely with high concentrations of limonene, linalool, hotrienol, α-terpineol, and myrcene, compared to wines from other grape varieties. An interesting observation regards the very strong correlations present between the two enantiomers of each compound, linalool and α-terpinyl ethyl ether in particular. This would hint at a very similar relative contribution in all wines of both enantiomers of all the three compounds (linalool and α-terpinyl ethyl ether in particular), and this may be related in our view to the findings about the formation of α-terpinyl ethyl ether reported in the following paragraph. The (*R*) enantiomeric excess for linalool, α-terpinyl ethyl ether, and α-terpineol (reported **in Table SI II-5**) are projected in the Loadings plot (as supplementary variables) in Fig. 4B. The enantiomeric excess for linalool was found to have higher values in 'Muscat' wines, while the enantiomeric excess for α-terpinyl ether was higher in 'Gewürztraminer' and in some 'Riesling' samples (RI 3, 5, and 6). The enantiomeric excess for α-terpineol was higher in 'Kerner', 'Lacrima di Morro d'Alba', and in some 'Riesling' samples (RI 2, 4, and 8). Notably, the enantiomeric excess variables were able to differentiate the varieties only to a small extent (*not shown*). Some studies have demonstrated instead that the enantiomeric ratios can be used as markers for grape variety (Furdíková et al., 2021; Song et al., 2018, 2022). To test the ability of these chemical compounds to differentiate the wines for the grape variety, regardless of the enantiomeric excesses, a linear discriminant analysis supervised classification was performed. As in the shown PCA (Fig. 4A) the three

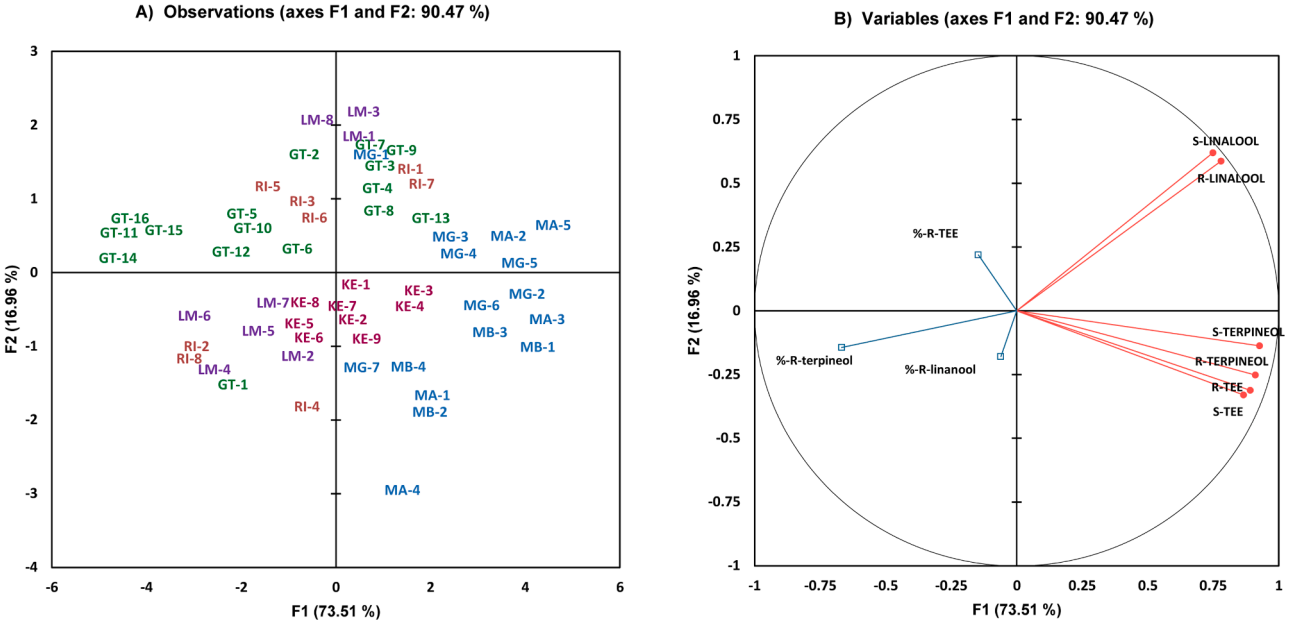

Fig. 4. Principal component analysis (PCA) of wines (Scores) from different varieties, applying $\log_{10}$-corrected and auto-scaled enantioselective-GCxGC-ToF/M(*S*)-measured relative abundances (peak areas) of the compounds as variables (Loadings). A) PC1 vs. PC2 Scores plot, and B) PC1 vs. PC2 Loadings plot. The blue vectors in B represent the (*R*) enantiomeric excesses of the compounds (projected as supplementary variables). Legend: KE1–6: 'Kerner', RI1–8: 'Riesling', MB1–4: 'Moscato Bianco', MA1–5: 'Muscat of Alexandria', MG1–7: 'Moscato Giallo', GT1–16: 'Gewürztraminer', LM1–8: 'Lacrima di Morro d'Alba'. TEE = α-terpinyl ethyl ether.

'Muscat' varieties clustered together very well, they were instead all grouped in a single class for LDA, to create a new class with a sample numerosity closer to that of other varietal classes. Considering the whole LDA model, 86.17±0.03 % of correct assignments in training and 88.89 ±0.08 % of correct assignments in validation were achieved (Table 3). By variety, considering specifically the validation step, 'Gewürztraminer' samples were correctly assigned on average 90.91±0.19 % of the times, 'Kerner' 100.00±0.00 %, 'Lacrima di Morro d'Alba' 89.39±0.18 %, 'Muscat' 95.45±0.14 %, and 'Riesling' 77.27±0.25 %. To evaluate the ability of the applied chemical variables to distinguish the three Muscat varietal groups, the MB, MG, and MA samples were separately analysed by variety in a second PCA model (**Figure SI II-17**). 'Moscato Giallo' wines were grouped differently than 'Muscat of Alexandria' and 'Moscato Bianco' wines, which instead presented similar distributions and trends.

3.6. Identification of potential terpene precursors of α-terpinyl ethyl ether isomers formation

To investigate potential precursors of α-terpinyl ethyl ether formation, (enantiomerically pure) (*R*)-linalool, (*R*)-limonene, and (*R*)-α-terpineol were individually spiked at 10 $mg{\cdot}L^{-1}$ and at 100 $mg{\cdot}L^{-1}$ in a synthetic model wine (composition: 7.5 $g{\cdot}L^{-1}$ L-tartaric acid, ABV 14 $\%_{v/v\ (aq.)}$, then pH set to 3.3 by titration with concentrated $KOH_{(aq.)}$). All spiked samples were prepared in duplicates and stored in darkness at 23 °C for 2 weeks. Then, the samples were analysed in enantioselective-GCxGC. Related chromatograms are shown in **Figure SI II-18 - 21** (only for the 100 $mg{\cdot}L^{-1}$ initially prepared concentrations) and the results are summarized in **Table SI II-6**. α-Terpineol and linalool resulted as direct precursors of α-terpinyl ethyl ether formation. α-(*R*)-terpineol showed only a small conversion after two weeks, and with no loss of the initial chiral configuration. (*R*)-linalool instead produced many degradation products (**Table SI II-6**), and with a much greater conversion (than with α-(*R*)-terpineol); from (*R*)-linalool, both enantiomers of α-terpineol and both enantiomers of α-terpinyl ethyl ether were among the most relatively abundant degradation products, in both cases with a predominant loss of the initial chiral configuration (close to racemates). Interestingly, from (*R*)-linalool, the enantiomeric excess of (*R*)-α-terpinyl ethyl ether was only 13±7 %, and the enantiomeric excess of (*R*)-α-terpineol was slightly higher at 25±2 %. Indeed, the found enantiomeric excesses of α-terpinyl ethyl ether and α-terpineol, although small, hinted at the presence of multiple degradation pathways, some of which may be partially enantioselective. Recent studies on the reactivity of linalool in wine showed a pathway to α-terpineol synthesis involving the formation of terpinolene (tentatively detected herein among the byproducts - **Table SI II-6**)(Yang et al., 2023). Terpinolene lacks an asymmetric centre (albeit being prochiral), and is thus an intermediate compatible with a conversion pathway involving a major or total loss of initial chiral configuration. Finally, the ratio between the molarities of α-terpinyl ethyl ether (sum of isomers) and α-terpineol (sum of isomers) was on average 17.1 ± 0.1 %. To gain a more complete view, the conversion from soluble linalool glycoside precursors should also be addressed in a future study, as this could contribute considerably to wine, depending on the specific vinification, fining, and storage time considered (Nicolini et al., 2003).

Furthermore, the degradation of (*S*)-α-terpinyl ethyl-d5 ether in the same conditions was also investigated. The application of the deuterated (*S*)-enantiomer analogue would allow investigation of the formation of (*S*)-α-terpineol from (*S*)-α-terpinyl ethyl-d5 ether, in order to indirectly test the reversibility of the α-terpineol conversion (to α-terpinyl ethyl ether). After two weeks, the main degradation products were (*S*)-limonene, (*S*)-α-terpineol (with full retention of chiral configuration), and terpinene. In summary, while (*R*)-α-terpineol converted into only the (*R*)-α-terpinyl ethyl ether isomer in two weeks at 0.01 $mg{\cdot}L^{-1}$, (*S*)-α-terpinyl ethyl-d5 ether converted only to the (*S*)-α-terpineol isomer at 0.17 $mg{\cdot}L^{-1}$: this discrepancy could also hint at other yet unexplored factors (e.g. the different reaction rates for the forward and backward reactions at this specific ethanol/water proportion, pH, and temperature). More tests should be carried out considering different ethanol/water ratios, different pH, different temperatures, and longer reaction times as well. Notably, both compounds produced over two weeks a similar quantity of the respective limonene enantiomer (0.58 $mg{\cdot}L^{-1}$) from an initial 100 $mg{\cdot}L^{-1}$ of precursor.

Table 3
Accuracies of the linear discriminant analysis (LDA) classification in training and validation (averaged over eleven calculated LDA models, each one with *prior* randomization and random extraction of a representative nine-sample validation set).

	Average number of correct assignments ± st.dev. (%)	
VARIETY	IN TRAINING	**IN VALIDATION**
GT	88.23±0.05	90.91±0.19
KE	87.01±0.10	100.00±0.00
LM	81.86±0.07	89.39±0.18
M	92.16±0.04	95.45±0.14
RI	70.13±0.10	77.27±0.25
TOTAL	86.17±0.03	88.89±0.08

Legend: GT- 'Gewürztraminer', KE - 'Kerner', LM - Lacrima, M – Muscat, and RI - 'Riesling'.

3.7. Qualitative determination of the olfactory attributes

A focus group was performed to provide a qualitative assessment of the olfactory descriptors associated with the α-terpinyl ethyl ether enantiomers. Samples of Pinot Blanc were spiked at different concentrations of either (*R*)-α-terpinyl ethyl ether, (*S*)-α-terpinyl ethyl ether, (*R*)-α-terpineol, and (*S*)-α-terpineol. A control wine (non-spiked Pinot Blanc wine matrix) was also provided. The results are presented as sum of frequency of the panel members that recognized the compounds spiked at different concentrations, for each compound independently (**Figure SI II-22**).

The resulting lexicons/descriptors is presented in **Figure SI II-23** as a word cloud in which the size of the words reflect the number of times the same descriptor was mentioned.

(*R*)-α-terpinyl ethyl ether could not differentiate the wines spiked at the lowest concentration (0.12 $mg{\cdot}L^{-1}$) from the control wine. However, 50 % of the panel members were able to recognize (*S*)-α-terpinyl ethyl ether and (*R*)-α-terpineol at the same concentration. Then, (*S*)-α-terpineol was recognized by almost all of the panel. At higher concentrations, > 75 % of the panellists (at 1.2 $mg{\cdot}L^{-1}$) or all the panellists (at 12 $mg{\cdot}L^{-1}$ and 120 $mg{\cdot}L^{-1}$) could perceive all compounds.

(*R*)-α-terpinyl ethyl ether was described as having an "earthy (mushroom)" aroma, followed by "herbaceous (fresh grass)", "pine", and "pome tree fruit (pear)" aromas; (*S*)-α-terpinyl ethyl ether was described mostly with "floral" aromas, followed by "chemical (cardboard)", "buttery", "pine", and "grass" notes (**Figure SI II-23**). The size of the words in the word clouds represents the frequency of the attributes provided by the panel. Sensory assessments in future studies should also consider mixtures of the α-terpinyl ethyl ether enantiomers at different ratios, as well as mixtures with other terpenes.

4. Conclusions

This study provides the analytical confirmation and profiling of α-terpinyl ethyl ether enantiomers in single-variety wines. Muscat wines ('Moscato Bianco', 'Moscato Giallo', and 'Muscat of Alexandria') had significantly higher concentrations of the quantified compounds compared to the other wines. Enantiomeric excesses were also calculated (for linalool, α-terpinyl ethyl ether, and α-terpineol): these values did not allow an accurate classification of the wines for the employed grape variety. On the contrary, the relative abundances of the specific compounds, applied as variables in LDA, provided accurate

classifications of the wines by the used grape variety, regardless of the producer, the *terroir*, the country of origin, or the vintage. Furthermore, limonene, linalool, and α-terpineol were investigated as potential precursors of α-terpinyl ethyl ether's formation. Linalool resulted the major precursor of α-terpinyl ethyl ether, but with almost complete loss of the original chiral configuration. From linalool, the obtained α-terpinyl ethyl ether (molar concentration of the sum of isomers) over two weeks was 17.1 ± 0.1 % that of α-terpineol (molar concentration of the sum of isomers), exceeding the ratio between ethanol and water for this process. Also α-terpineol converted to α-terpinyl ethyl ether, but this process presented a much smaller conversion over the same time than from linalool and no observable loss of chiral configuration. By applying a synthesized deuterated ethyl ether analogue (α-terpinyl ethyl-d5 ether) as the precursor in the same experimental conditions, the (inter)conversion from α-terpineol was also proved to be fully reversible. The found reversibility would suggest that the ratio between α-terpinyl ethyl ether and α-terpineol should reach an equilibrium overtime defined mainly by the ratio between ethanol and water in wine. However, in the real tested wines, the concentration of α-terpinyl ethyl ether was much lower than that of α-terpineol, regardless of the alcohol-to-water ratio, which may hint at more than one formation pathways of α-terpinyl ethyl ether in wine, or at yet unexplored possible precursors (e.g. terpene glycosides precursors). Indeed, given the found reversibility of the conversion from α-terpineol, the concentrations found in the wines for α-terpinyl ethyl ether were overall surprisingly much lower than those of α-terpineol, only slightly dependent on the ethanol-water ratio, and not significantly dependent from the wine age. In future studies, longer-aged wines (especially aromatic) should be tested, to investigate if the ratio between α-terpinyl ethyl ether and α-terpineol does eventually reach an equilibrium set by the wine's ethanol-water ratio.

Finally, qualitative olfactory attributes for each α-terpinyl ethyl ether enantiomer spiked in a neutral white wine (Pinot Blanc) were qualitatively assigned: (*R*)-α-terpinyl ethyl ether was described with "earthy (mushroom)", "herbaceous (fresh grass)", "pine", and "pome tree fruit (pear)" aromas; (*S*)-α-terpinyl ethyl ether was described with "floral", "chemical (cardboard)", "buttery", "pine", and "grass" aromas. Sensory assessments in future studies should also consider mixtures of the α-terpinyl ethyl ether enantiomers at different ratios, as well as mixtures with other terpenes, as this could likely induce different attributes and odour potencies than those displayed by the individual enantiomers.

Supporting information

Paragraph I.1. Synthesis of (*S*)-α-terpinyl ethyl ether; Figure SI I-1. Scheme of the synthesis of (*S*)-α-terpinyl ethyl ether; Paragraph I.2. Synthesis of (*R*)-α-terpinyl ethyl ether; Figure SI I-2. Scheme of the synthesis of (*R*)-α-terpinyl ethyl ether; Paragraph I.3. Synthesis of (*S*)-α-terpinyl ethyl-d5 ether; Figure SI I-3. Scheme of the synthesis of (*S*)-α-terpinyl ethyl-d5 ether; Paragraph II.1. Characterization of the synthesized (*S*)-α-terpinyl ethyl ether; Figure SI II-1. Normalized eGC-ToF/MS TIC trace of (*S*)-α-terpinyl ethyl ether after flash chromatography purification; Figure SI II-2. Direct injection APCI-(HR)MS/MS for (*S*)-α-terpinyl ethyl ether; Figure SI II-3. APCI-(HR)MS/MS tentatively proposed fragmentation mechanism for (*S*)-α-terpinyl ethyl ether and (*R*)-α-terpinyl ethyl ether; Figure SI II-4. FTIR transmittance (%) spectrum of (*S*)-α-terpinyl ethyl ether pure standard; Paragraph II.2. Characterization of the synthesized (*R*)-α-terpinyl ethyl ether; Figure SI II-5. Normalized eGC-ToF/MS TIC trace of (*R*)-α-terpinyl ethyl ether after flash chromatography purification. Inset: acquired EI-MS spectrum; Figure SI II-6. Direct injection APCI-(HR)MS/MS for (*R*)-α-terpinyl ethyl ether; Figure SI II-7. FTIR transmittance (%) spectrum of (*R*)-α-terpinyl ethyl ether pure standard; Paragraph II.3. Characterization of the synthesised (*S*)-α-terpinyl ethyl-d5 ether; Figure SI II-8. Normalized eGC-ToF/MS TIC trace of (*S*)-α-terpinyl ethyl-d5 ether after flash chromatography purification; Figure SI II-9. Direct injection APCI-(HR)MS/MS for (*S*)-α-terpinyl ethyl-d5 ether; Figure SI II-10. APCI-(HR)MS/MS tentatively proposed fragmentation mechanism for (*S*)-α-terpinyl ethyl-d5 ether; Figure SI II-11. FTIR transmittance (%) spectrum of (*S*)-α-terpinyl ethyl-d5 ether pure standard; Figure SI II-12. Portions of the HS-SPME-enantioselective-GCxGC-ToF/MS AIC traces for the spiked Pinot Blanc wine, and the non-spiked Pinot Blanc wine; Figure SI II-13. AIC traces from HS-SPME-enantioselective-GCxGC-ToF/MS analysis of (*S*)-α-terpinyl ethyl ether and (*R*)-α-terpinyl ethyl ether isomers spiked in a wine already naturally containing these compounds; Figure SI II-14. Extracted ion chromatograms (XIC) traces for the HS-SPME-enantioselective-GCxGC-ToF/MS analysis; Figure SI II-15. 1H and 13C NMR chemical shift assignments of (*S*)-α-terpinyl ethyl ether and (*S*)-α-terpinyl ethyl-d5 ether; Table SI II-1. Calibration parameters; Table SI II-2. Precision and recovery; Table SI II-3. Evaluation of robustness of the method; Table SI II-4. Varietal matrix effect presented as significance; Table SI II-5. Enantiomeric excesses for linalool, α-terpinyl ethyl ether (TEE), α-terpineol (Terp); Figure SI II-17. Principal Component Analysis (PCA) biplot for Muscat wine samples; Figure SI II-18. HS-SPME-enantioselective-GCxGC-ToF/MS chromatogram (AIC) of the synthetic model wine solution added with (*R*)-α-terpineol; Figure SI II-19. HS-SPME-enantioselective-GCxGC-ToF/MS chromatogram (AIC) of the synthetic model wine solution added with (*R*)-limonene; Figure SI II-20. HS-SPME-enantioselective-GCxGC-ToF/MS chromatogram (AIC) of the synthetic model wine solution added with (*R*)-linalool; Figure SI II-21. HS-SPME-enantioselective-GCxGC-ToF/MS chromatogram (AIC) of (*S*)-α-terpinyl ethyl-d5 ether; Table SI II-6. Investigated potential wine terpene precursors for α-terpinyl ethyl ether with their observed degradation products; Figure SI II-22. The sum of the frequency of the panellists that recognized the compounds at different concentrations; Figure SI II-23. Word clouds for (*R*)-α-terpinyl ethyl ether, (*S*)-α-terpinyl ethyl ether, (*R*)-α-terpineol, and (*S*)-α-terpineol.

Funding

The present works was partially funded on the project 'RGTan' (TN221K, by the 'Società Italiana di Scienze e Tecnologie Alimentari' - S.I.S.T.A.L.), Onfoods PNRR (TN221U), and Ph.D. scholarship funds unibz. The Autonomous Province of Bozen-Bolzano, Department of Innovation, Research and University is gratefully acknowledged for financial support of the enology laboratory (Oenolab) within the 'AMARE' Capacity Building and the Laboratory of NMR Spectroscopy within the NOI Capacity building I and II funding frame (Decision n. 1472, 07.10.2013; Decision n. 864,04.09.2018). Laimburg Research Centre is funded by the Autonomous Province of Bozen-Bolzano. This publication has been supported by the Open-Access fund from the library of the Free University of Bozen - Bolzano.

Ethical statement

The authors confirm that the appropriate protocols for protecting the rights and privacy of all participants were utilized during the execution of the research, including no coercion to participate, full disclosure of study requirements and risks, consent of participants, no release of participant data without their knowledge, and the ability to withdraw from the study at any time.

CRediT authorship contribution statement

Aakriti Darnal: Writing – original draft, Visualization, Validation, Methodology, Investigation, Formal analysis, Data curation. **Alberto Ceccon:** Writing – review & editing, Writing – original draft, Visualization, Validation, Resources, Methodology, Investigation, Formal analysis, Data curation, Conceptualization. **Martina Magni:** Writing – review & editing, Validation, Methodology, Investigation. **Peter Robatscher:** Writing – review & editing, Supervision, Resources. **Simone Poggesi:** Writing – review & editing, Investigation. **Emanuele Boselli:** Writing – review & editing, Supervision, Resources, Funding

acquisition. **Edoardo Longo:** Writing – review & editing, Validation, Supervision, Project administration, Methodology, Investigation, Funding acquisition, Conceptualization, Data curation, Formal analysis, Resources, Visualization, Writing – original draft.

Declaration of competing interest

The authors declare that they have no known competing financial interests or personal relationships that could have appeared to influence the work reported in this paper.

Data availability

Data will be made available on request.

Acknowledgment

The authors would like to thank Prof. Carlo Bicchi (Department of Drug Science and Technology, University of Torino, Italy) for the kind suggestions for developing enantioselective-bidimensional gas chromatography methods and the related stationary phases. The authors want to thank MEGA S.r.l. (Legnano, Milano, Italy) for their support with the screening of stationary phases. The authors would like to thank also Dr. Vittoria Benedetti (Free University of Bozen-Bolzano), Bruno Plasinger (Fachoberschule für Landwirtschaft Auer, Auer/Ora, Italy), and Giulia Windisch (Free University of Bozen-Bolzano) for their support with the analyses. Finally, our gratitude goes to all panellists that have voluntarily participated in the qualitative olfactory sensory assessment.

Supplementary materials

Supplementary material associated with this article can be found, in the online version, at doi:10.1016/j.afres.2024.100538.

References

Black, C. A., Parker, M., Siebert, T. E., Capone, D. L., & Francis, I. L. (2015). Terpenoids and their role in wine flavour: Recent advances. *Australian Journal of Grape and Wine Research, 21*, 582–600. https://doi.org/10.1111/AJGW.12186

Blackford, C. L., Trengove, R. D., & Boss, P. K. (2022). Exploring the influence of grape tissues on the concentration of wine volatile compounds. *Australian Journal of Grape and Wine Research, 28*(2), 218–231. https://doi.org/10.1111/ajgw.12524

Boselli, E., Giomo, A., Minardi, M., & Frega, N. G. (2008). Characterization of phenolics in Lacrima di Morro d'Alba wine and role on its sensory attributes. *European Food Research and Technology, 227*(3), 709–720. https://doi.org/10.1007/S00217-007-0777-7/FIGURES/7

Burger, R., & Bigler, P. (1998). DEPTQ: Distorsionless enhancement by polarization transfer including the detection of quaternary nuclei. *Journal of Magnetic Resonance, 135*(2), 529–534. https://doi.org/10.1006/JMRE.1998.1595

Büyükbayram, M., Gürer, S., Çat, Y., Canayakın, O., Altuğ, C., & Sağırlı, A. (2024). Design, synthesis, olfactory evaluation and molecular docking study of Isoxazoline carboxylate derivatives as fragrance molecules. *Flavour and Fragrance Journal*. https://doi.org/10.1002/FFJ.3778

Carlin, S., Vrhovsek, U., Franceschi, P., Lotti, C., Bontempo, L., Camin, F., et al. (2016). Regional features of northern Italian sparkling wines, identified using solid-phase micro extraction and comprehensive two-dimensional gas chromatography coupled with time-of-flight mass spectrometry. *Food Chemistry, 208*, 68–80. https://doi.org/10.1016/j.foodchem.2016.03.112

Catrinescu, C., Fernandes, C., Castilho, P., & Breen, C. (2015). Selective methoxylation of α-pinene to α-terpinyl methyl ether over Al3+ ion-exchanged clays. *Applied Catalysis A: General, 489*(1), 171–179. https://doi.org/10.1016/J.APCATA.2014.10.028

Chambers, P. J., & Pretorius, I. S. (2010). Fermenting knowledge: The history of winemaking, science and yeast research. *EMBO Reports, 11*(12), 914. https://doi.org/10.1038/EMBOR.2010.179

Silva, Da, J, M., Carari, D. M., & Silva, Manoel Da (2015). Fe(III)-catalyzed α-terpinyl derivatives synthesis from β-pinene via reactions with hydrogen peroxide in alcoholic solutions. *RSC Advances, 5*(14), 10529–10536. https://doi.org/10.1039/C4RA13112F

da Silva, M. J., de Andrade Leles, L. C., & Teixeira, M. G. (2020). Lewis acid metal cations exchanged heteropoly salts as catalysts in β-pinene etherification. *Reaction Kinetics, Mechanisms and Catalysis, 131*(2), 875–887. https://doi.org/10.1007/S11144-020-01888-4/FIGURES/10

Falcao, L. D., Lytra, G., Darriet, P., & Barbe, J. C. (2012). Identification of ethyl 2-hydroxy-4-methylpentanoate in red wines, a compound involved in blackberry aroma. *Food Chemistry, 132*(1), 230–236. https://doi.org/10.1016/J.FOODCHEM.2011.10.061

Furdíková, K., Khvalbota, L., Machyňáková, A., & Špánik, I. (2021). Volatile composition and enantioselective analysis of chiral terpenoids in Tokaj varietal wines. *Journal of Chromatography B, 1167*, Article 122565. https://doi.org/10.1016/J.JCHROMB.2021.122565

Gao, J., Owen, B. C., Borton, D. J., Jin, Z., & Kenttämaa, H. I. (2012). HPLC/APCI mass spectrometry of saturated and unsaturated hydrocarbons by using hydrocarbon solvents as the APCI reagent and HPLC mobile phase. *Journal of the American Society for Mass Spectrometry, 23*(5), 816–822. https://doi.org/10.1007/S13361-012-0347-5/FIGURES/2

Gilles, L., & Antoniotti, S. (2022). Spirocyclic compounds in fragrance chemistry: Synthesis and olfactory properties. *ChemPlusChem, 87*(11), Article e202200227. https://doi.org/10.1002/CPLU.202200227

González-Barreiro, C., Rial-Otero, R., Cancho-Grande, B., & Simal-Gándara, J. (2015). Wine aroma compounds in grapes: A critical review. *Critical Reviews in Food Science and Nutrition, 55*(2), 202–218. https://doi.org/10.1080/10408398.2011.650336

Hensen, K., Mahaim, C., & Hölderich, W. F. (1997). Alkoxylation of limonene and alpha-pinene over beta zeolite as heterogeneous catalyst. *Applied Catalysis A: General, 149*(2), 311–329. https://doi.org/10.1016/S0926-860X(96)00273-6

Keyzers, R. A., & Boss, P. K. (2010). Changes in the volatile compound production of fermentations made from musts with increasing grape content. *Journal of Agricultural and Food Chemistry, 58*(2), 1153–1164. https://doi.org/10.1021/JF9023646/SUPPL_FILE/JF9023646_SI_001.PDF

Khvalbota, L., Machyňáková, A., Čuchorová, J., Furdíková, K., & Špánik, I. (2021). Enantiomer composition of chiral compounds present in traditional Slovak Tokaj wines. *Journal of Food Composition and Analysis, 96*, Article 103719. https://doi.org/10.1016/J.JFCA.2020.103719

Langen, J., Wegmann-Herr, P., & Schmarr, H. G. (2016). Quantitative determination of α-ionone, β-ionone, and β-damascenone and enantiodifferentiation of α-ionone in wine for authenticity control using multidimensional gas chromatography with tandem mass spectrometric detection. *Analytical and Bioanalytical Chemistry, 408*(23), 6483–6496. https://doi.org/10.1007/S00216-016-9767-6/TABLES/4

Li, C., Sun, J., Fu, C., Yu, B., Liu, S. Q., Li, T., et al. (2014). Synthesis and evaluation of odour-active methionyl esters of fatty acids via esterification and transesterification of butter oil. *Food Chemistry, 145*, 796–801. https://doi.org/10.1016/J.FOODCHEM.2013.08.124

Nicolini, G., Versini, G., Moser, S., Carlin, S., & Malossini, U. (2003). Aroma characteristics of wines from the cultivar "Manzoni bianco" ("White Riesling" x 'Pinot blanc'). *Mitteilungen Klosterneuburg, 53*, 251–257.

Pineau, B., Barbe, J. C., Van Leeuwen, C., & Dubourdieu, D. (2007). Which impact for β-damascenone on red wines aroma? *Journal of Agricultural and Food Chemistry, 55*(10), 4103–4108. https://doi.org/10.1021/JF070120R

Poggesi, S., Darnal, A., Ceci, A. T., Longo, E., Vanzo, L., Mimmo, T., et al. (2022). Fusion of 2DGC-MS, HPLC-MS and sensory data to assist decision-making in the marketing of international monovarietal chardonnay and sauvignon blanc wines. *Foods (Basel, Switzerland), 11*(21), 3458. https://doi.org/10.3390/FOODS11213458/S1

Polo, H. P., Lopes, N. P. G., & da Silva, M. J. (2019). Exploring the Keggin-type heteropolyacid-catalyzed reaction pathways of the β-pinene with alkyl alcohols. *Catalysis Letters, 149*(10), 2844–2853. https://doi.org/10.1007/s10562-019-02808-5

Praet, T., Van Opstaele, F., Steenackers, B., De Brabanter, J., De Vos, D., Aerts, G., et al. (2015). Changes in the hop-derived volatile profile upon lab scale boiling. *Food Research International, 75*, 1–10. https://doi.org/10.1016/j.foodres.2015.05.022

Qin, D., Lv, S., Shen, Y., Shi, J., Jiang, Y., Cheng, W., et al. (2024). Decoding the key compounds responsible for the empty cup aroma of soy sauce aroma type baijiu. *Food Chemistry, 434*, Article 137466. https://doi.org/10.1016/J.FOODCHEM.2023.137466

Sensory Properties of Optical Isomers | Perfumer & Flavorist. (n.d.). Retrieved April 5, 2024, from https://www.perfumerflavorist.com/flavor/ingredients/article/21860886/sensory-properties-of-optical-isomers.

Song, M., Fuentes, C., Loos, A., & Tomasino, E. (2018). Free monoterpene isomer profiles of Vitis Vinifera L. cv. white wines. *Foods (Basel, Switzerland), 7*(2). https://doi.org/10.3390/FOODS7020027

Song, M., Fuentes, C., & Tomasino, E. (2022). Chemo-diversity of chiral monoterpenes in different styles of Riesling wine from different regions. *OENO One, 56*(3), 155–165. https://doi.org/10.20870/OENO-ONE.2022.56.3.4834

Strauss, C. R., & Williams, P. J. (1983). The effect of distillation on grape flavour components. In *Flavour of Distilled Beverages Symposium 1-4th June*. Scotland: Univ. of Stirling.

Strauss, C. R., Wilson, B., Williams, P. J., Rapp, A., & Guentert, M. (1985a). New monoterpene ethyl ethers in grape wines and brandies. *Journal of Agricultural and Food Chemistry, 33*(4), 706–708. https://doi.org/10.1021/JF00064A034/ASSET/JF00064A034.FP.PNG_V03

Strauss, C. R., Wilson, B., Williams, P. J., Rapp, A., & Guentert, M. (1985b). New monoterpene ethyl ethers in grape wines and brandies. *Journal of Agricultural and Food Chemistry, 33*(4), 706–708. https://doi.org/10.1021/jf00064a034

Tomasino, E., Song, M., & Fuentes, C. (2020). Odor perception interactions between free monoterpene isomers and wine composition of pinot gris wines. *Journal of Agricultural and Food Chemistry, 68*(10), 3220–3227. https://doi.org/10.1021/ACS.JAFC.9B07505/ASSET/IMAGES/LARGE/JF9B07505_0002.JPEG

Uehara, A., & Baldovini, N. (2021). Stereoselective synthesis of (6Z,8E)-undeca-6,8,10-trien-3-one (yuzunone) for its characterization in yuzu and various citrus essential oils. *Food Chemistry, 338*, Article 128130. https://doi.org/10.1016/J.FOODCHEM.2020.128130

Versini, G., Dellacassa, E., Carlin, S., Fedrizzi, B., & Magno, F. (2008). *Analysis of aroma compounds in wine*. 173–225. https://openpub.fmach.it/handle/10449/17031.

Wedler, H. B., Pemberton, R. P., & Tantillo, D. J. (2015). Carbocations and the complex flavor and bouquet of wine: mechanistic aspects of terpene biosynthesis in wine grapes. *Molecules (Basel, Switzerland), 20*(6), 10781–10792. https://doi.org/10.3390/MOLECULES200610781. *2015, Vol. 20, Pages 10781-10792*.

Yang, Y., Frank, S., Wei, X., Wang, X., Li, Y., Steinhaus, M., et al. (2023). Molecular rearrangement of four typical grape free terpenes in the wine environment. *Journal of Agricultural and Food Chemistry, 71*(1), 721–728. https://doi.org/10.1021/ACS.JAFC.2C07576/ASSET/IMAGES/LARGE/JF2C07576_0005.JPEG

Zhu, J. C., Zhu, Y., Wang, K., Niu, Y. W., & Xiao, Z. B. (2021). Characterization of key aroma compounds and enantiomer distribution in Longjing tea. *Food Chemistry, 361*, Article 130096. https://doi.org/10.1016/J.FOODCHEM.2021.130096